JOTCS A
Journal of the Turkish Chemical Society Section: A Chemistry
TURKISH CHEMICAL SOCIETY

A Highly Sensitive Non-Enzymatic Sensor for the Determination of Glucose Based on Aniline-2-sulfonic acid-Modified Cu Electrode

Melih Besir Arvas[1*]

[1]Istanbul University Department of Chemistry, Istanbul, 34134, Turkey

Abstract: Herein, the copper-based electrodes were successfully synthesized with galvanostatic electrodeposition method. The effect of materials obtained at different concentrations of ASA and anodization times on glucose sensing ability was investigated. During the anodization of copper foil in the presence of ASA molecules, it formed a tree branch-like structure connected to each other while decorating the electrode surface. The Cu(30)/ASA(0.02) electrode exhibited a relatively wide linear range (0.2 – 10.0 mM) and a low detection limit (0.826 µM). These excellent activities were mainly attributed to the surface morphology, which functions as highly active sites and enhanced electronic conductive pathways with the addition of ASA. In addition, the stability obtained together with the excellent sensing ability in beverages makes the electrodes useful for practical applications.

Keywords: Copper foil, anodization method, glucose, non-enzymatic sensor, aniline 2-sulfonic acid.

Submitted: October 01, 2022. **Accepted:** December 26, 2022.

Cite this: Arvas MB. A Highly Sensitive Non-Enzymatic Sensor for the Determination of Glucose Based on Aniline-2-sulfonic acid-Modified Cu Electrode. JOTCSA. 2023;10(1):227–40.

DOI: https://doi.org/10.18596/jotcsa.1182942.

***Corresponding author. E-mail:** mbesirarvas@gmail.com.

1. INTRODUCTION

In various industries, such as clinical diagnosis, medicine, and the food business, it is critical to create fast, practical, and reliable methods for determining glucose. Because most diabetics are unaware of the early indicators of the condition, regular blood sugar monitoring and exact detection are essential for diagnosing and controlling this life-threatening disease. Because of their excellent sensitivity and selectivity, most electrochemical glucose biosensors on the market today are made primarily with the glucose oxidase enzyme for blood glucose detection in various body fluids (1–3). However, enzymatic glucose sensors have some drawbacks, such as enzyme denaturation, high cost, low chemical stability, and expensive manufacturing methods, hence enzyme-free glucose sensors are being developed to replace enzymatic glucose sensors. Enzyme-free glucose sensors appear to be a promising alternative to enzyme-based glucose sensors, although existing non-enzymatic glucose sensors still require significant sensitivity and selectivity improvements. Researchers are particularly interested in studies that focus on developing stable, simple, repeatable, low-cost non-enzymatic glucose sensors and synthesizing more sensitive materials.

Non-enzymatic electrodes, such as electrodes modified with noble metals, metal alloys, and metal nanoparticles, have been developed with a lot of effort (4–9). Copper and copper oxide-based materials, for example, are low-cost, non-toxic semiconductors with good electrochemical and catalytic characteristics (10). By adjusting the process conditions, different morphologies of copper and copper oxide-based materials can be synthesized using simple procedures (11). Furthermore, their nanostructures have distinct characteristics, such as a large surface area, low density, and the existence of active sites even on the interior surfaces (12,13). Previous research has looked into copper and copper oxide-based materials' high catalytic activity in alkaline solutions for glucose detection. Jiang et al. described a non-enzymatic glucose sensor electrode made of Cu NPs with nitrogen-doped graphene as the sensing

component (14). Zhang et al. used a simple substrate-assisted electroless deposition (SAED) process to create a flexible enzyme-free glucose amperometric biosensor on free-standing reduced graphene oxide (rGO) membranes using a laser-induced graphene (Cu NPs-LIG) composite (15). Anand et al. reported a sensitive nonenzymatic glucose sensor based on copper nanowires (CuNWs)/polyaniline (PANI)/reduced graphene oxide (rGO) nanocomposite ink by solvothermal mixing of CuNWs, PANI, rGO and binders (16). Phetsang et al. developed a non-enzymatic glucose sensor based on a screen-printed carbon electrode modified with copper(II) and reduced graphene oxide (17). Controllable morphology investigations are carried out with the doped form formed by adding a dopant in order to improve the sensitivity of the copper-based glucose sensor. Aniline 2-sulfonic acid (ASA) may be promising as a dopant with sulfo groups because the sulfonic acid group is defined by the maximum degree of dissociation (18,19). Because of the sulfo groups and nitrogen atoms in the monomer chain structure, aniline 2-sulfonic acid (ASA) has not yet been explored as a doping at copper electrode material (20).

We used a simple one-step anodization procedure to make tree branch-shaped CuO–Cu_2O/copper/aniline 2-sulfonic acid directly on copper foil. The synthesis technique, which uses copper foil as both a current collector and a copper source, simplifies electrode fabrication while simultaneously increasing charge efficiency with additives for increased sensor sensitivity. Scanning electron microscopy (SEM), energy distribution spectrum (EDS), X-ray diffraction (XRD), Fourier-transform infrared spectroscopy (FT-IR), and electrochemical tests were used to characterize the aniline 2-sulfonic acid modified copper foil electrode. Compared to Cu(30) electrodes and many other non-enzymatic glucose sensors, the Cu(30)/ASA/(0.03) electrode for glucose sensors has good electrocatalytic capabilities for glucose oxidation and detection. This new electrode material, which takes advantage of ASA's functional groups, promises to be an outstanding non-enzymatic glucose sensor with high sensitivity, excellent selectivity, a wide detection range, and excellent surface properties.

2. EXPERIMENTAL

2.1. Chemicals and Reagents

Acetone (C_3H_6O, ≥99.9%), ethanol absolute (C_2H_5OH, ≥97.9%), sodium hydroxide (NaOH, ≥97.0%), copper(II) sulfate pentahydrate ($CuSO_4 \cdot 5H_2O$, ≥98.0%), were purchased from Sigma Aldrich. Copper foil (99.9%) was provided by Alfa Aesar. All beverage samples were obtained from the local market for real samples analysis. Distilled water (Milli-Q, 18 MΩ.cm resistivity) was used to prepare all the aqueous solutions.

2.2. Synthesis of Tree Branch-Shaped CuO–Cu_2O/copper/aniline-2-sulfonic acid Electrode

The electrodes were prepared by controlled galvanostatic electrodeposition method. Copper electrodes were cleaned with ethanol, acetone, deionized water in the ultrasonic bath for 15 min to remove contaminants on the electrode surface and dried at the room temperature overnight, respectively. In a typical synthesis procedure, a constant current of 0.5 A cm^{-2} is applied for 30 s in a two-electrode cell. Cu foil (1×3 cm^2) was used as a cathode electrode for the electrochemical deposition and another piece of Cu foil used as an anode electrode. The effect of electrochemical deposition time on the growth of the copper oxides was investigated at anodization times of 10, 20, 30, 40 and 50 second in 0.4 M $CuSO_4$ and 1.5 M H_2SO_4 electrolyte solution. Then, CuO–Cu_2O/copper/aniline 2-sulfonic acid electrodes were prepared under similar electrochemical conditions by adding in the presence of between 0.005, 0.01, 0.02, 0.03, 0.04, 0.05 M ASA concentration (see Table 1). The prepared electrodes were thoroughly rinsed with distilled water and ethanol several times, and dried in an oven at 60 °C for 3 hours. The obtained electrodes were used as the sensing material for sensitive glucose detection.

2.3. Characterization

Scanning electron microscopy (SEM) and energy distribution spectrum (EDS) were used to examine the surface morphologies and elemental analyses of the electrodes prepared using Zeiss EVO® LS 10 SEM, USA. Fourier-transform infrared spectroscopy (FT-IR) for the analysis of chemical structure was recorded Perkin Elmer Spectrum 100 spectrophotometer. X-RAY diffractometer (XRD, PANalytical X'Pert PRO Cu) at 45 kV and 2θ range of 10-80^0 was used to determine the phase and crystallinity of the structures coated on the electrode surface.

2.4. Electrochemical Measurements

All electrodes were tested using Ivium Vertex Instruments Potentiostat/Galvanostat (Ivium Technologies B.V, Netherlands) and recorded with the IviumSoft Potentiostat/Galvanostat software. The electrochemical sensor was carried out based on four methods in applications, cyclic voltammetry (CV), differential pulse voltammetry (DPV), chronoamperometry (CA) and electrochemical impedance spectroscopy (EIS). In the presence of probable interfering substances such as ascorbic acid, lactic acid, uric acid, maltose, lactose, and urea, the selectivity of the sensor electrode was studied.

Table 1: The ratio of raw materials used in sensor electrode samples.

Sample	Anodization Time (s)	ASA (M)
Cu	-	-
Cu(10)	10.0	-
Cu(20)	20.0	-
Cu(30)	30.0	-
Cu(40)	40.0	-
Cu(50)	50.0	-
Cu(30)/ASA/(0.005)	30.0	0.005
Cu(30)/ASA/(0.01)	30.0	0.01
Cu(30)/ASA/(0.02)	30.0	0.02
Cu(30)/ASA/(0.03)	30.0	0.03
Cu(30)/ASA/(0.04)	30.0	0.04
Cu(30)/ASA/(0.05)	30.0	0.05

2.5. Preparation of Real Samples

All beverage samples were obtained from local shops for real sample analysis. In order to detect glucose in real samples by electrochemical methods, beverage samples such as cola, fruit juice and ice tea were placed directly into the test cell. To perform the sensor sensitivity of electrode, 10 mL of NaOH (0.1 M) electrolyte was added so that the real sample concentrations were 5.0 mM.

3. RESULTS AND DISCUSSION

As the material has highly porous interfaces, it is a promising material for sensor electrodes. The sensor properties of this material produced at different anodization times were systematically tested using cyclic voltammetry measurement. The electrochemical properties of copper samples were investigated with a cyclic voltammetry (CV) method in 1.0 M NaOH solution within presence of 5 mM glucose in a potential window of –0.2 V to 1.0 V with scan rate of 50 mV s^{-1}. Figure 1a shows that all electrodes had an oxidation peak in the region of 0.3–0.6 V, which can be attributed to Cu(II) to Cu(III) conversion. Kuwana et al. reported the most widely accepted method of glucose oxidation at the CuO electrode in an alkaline media (21). Cu(III) oxidation could catalyse glucose oxidation to gluconolactone, which could then be further oxidized to glucose acid (22). Among all the electrodes, Cu(30) showed the highest anodic current peak indicating the highest electrocatalytic performance. As shown in Figure 1a the cyclic voltammograms of anodized copper in various times, 30 seconds was obtained as the optimum time as Cu oxidized at that time and it improved the surface properties of the sensor. In order to improve the electrochemical performance of Cu(30) electrodes, the electrodes were anodized in the presence of ASA concentration and cyclic voltammetry (CV) and electrochemical impedance spectroscopy (EIS) measurements were used to investigate the effect of ASA in Figure 1b and 1c.

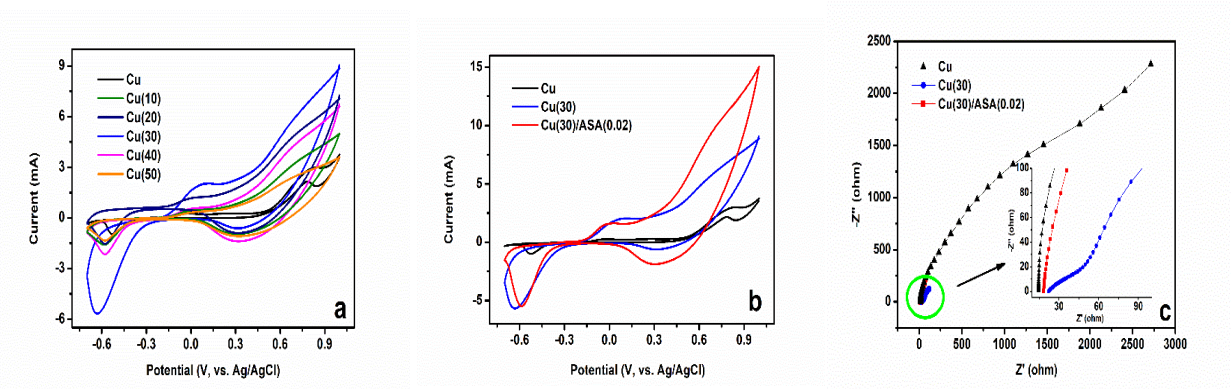

Figure 1: (a) Cyclic voltammograms of the copper electrodes in 1.0 M NaOH in presence of 5 mM glucose with scan rate of 50 mV s^{-1}; (b) Cyclic voltammograms of the Cu, Cu(30) and Cu(30)/ASA(0.02) electrodes in 1.0 M NaOH in presence of 5 mM glucose with scan rate of 50 mV s^{-1}; (c) Electrochemical impedance spectra of the Cu, Cu(30) and Cu(30)/ASA(0.02) electrodes in 1.0 M NaOH in presence of 5 mM glucose the inset is the enlarged with region of the high frequency.

With the synthesized Cu(30)/ASA(0.02) electrode, ASA improved the electrochemical activity and surface area, and the corresponding cyclic voltammograms were shown in Figure 1b. The sensor Cu(30)/ASA(0.02) electrode with higher electrochemical properties has more activity than

anodized Cu(30) and bare copper (Cu) electrode sensors. The ASA modified electrode acted as electron mediators, enhancing the synergistic effect. Thus, the selectivity of the electrode against the glucose was improved. This result can also be related to the porous structure of the Cu(30)/ASA(0.02) electrode's wide surface area following anodization with the addition of ASA to the medium.

Figure 1c showed the electrochemical impedance spectra (EIS) of Cu, Cu(30) and Cu(30)/ASA(0.02) electrodes in 0.1 M NaOH solution from 0.01 Hz to 10000 Hz. The resulting Nyquist curves were fitted according to the equivalent simple circuit model. Solution resistance, charge transfer resistance, double layer capacitance, and Warburg impedance are represented by the impedances Rs, Rct, Cdl, and W, respectively. Rs is the ohmic resistance and is the resistivity of the electrolyte and corrosion products on the surface. Rct, on the other hand, was linked to the velocity resistance that governs the corrosion reaction. W is connected to the diffusion rate of mobile ions to the electrode surface, whereas Cdl is related to the capacitive behaviour of the electrodes. The Rs values of Cu, Cu(30) and Cu(30)/ASA(0.02) electrodes were 15.73 Ω , 22.76 Ω and 17.83 Ω, respectively. After anodization of copper for 30 seconds, the Rs value of the Cu(30)/ASA(0.02) electrode synthesized by adding ASA to the anodization medium was lower. The Rct values of Cu, Cu(30) and Cu(30)/ASA(0.02) electrodes were 1338 Ω, 47.68 Ω and 23.49 Ω, respectively. The Rct value of the Cu(30)/ASA(0.02) electrode obtained after the anodization process with the addition of ASA decreased by almost half compared to the Cu(30) electrode. The Cdl values of Cu, Cu(30) and Cu(30)/ASA(0.02) electrodes were 34.89e-6, 110.4e-6 and 124.7e-6, respectively. When the electrode was anodized with ASA for 30 seconds, the capacitive behaviour of the electrode improved. Cu, Cu(30), and Cu(30)/ASA(0.02) electrodes had W impedance values of 17.31e-3, 4.33e-3, and 14.39e-3, respectively. The sulfonyl groups in ASA had a favourable effect on electrode surface, lowering charge transfer resistance and accelerating ion diffusion rates. As a result, electron transfer on the electrode surface was accelerated, and the electrode's selectivity against the analyte was enhanced. The influence of the ASA concentration on the anodization of copper electrode for sensor applications was investigated using cyclic voltammetry and electrochemical impedance spectroscopy. Figure 2a shows a comparison of electrochemical tests utilizing a three-electrode system in 0.1 M NaOH electrolyte from a -0.7 V to 1.0 V potential window with a scan rate of 50 mV s^{-1} in the presence of ASA concentrations ranging from 0.005 to 0.05 M. At the cyclic voltammogram, the Cu(30)/ASA(0.02) containing 0.02 M ASA showed the maximum current density rise.

To consider the electrocatalytic activity between the electrodes due to the concentration difference, the higher catalytic activity of Cu(30)/ASA(0.02) could be attributed to two reasons. First, it could be that the Cu(30)/ASA(0.02) electrode has high electrode surface area due to the well-dispersed negative charge of ASA during its synthesis. Because ASA contains sulfonic acids with a high protonation degree and electrical conductivity characteristics in its molecular structure (23–25). Therefore, it may have raised the deposition efficiency of copper oxide on the electrode surface, which was directly related to its catalytic activity on glucose oxidation. The addition of less or more 0.02 M ASA, on the other hand, may have resulted in decreased copper oxide electrocatalytic activity for glucose oxidation. As a result, the ASA content in the Cu(30) electrodes was optimized to 0.02 M.

Figure 2b shows the Nyquist curves of EIS analyses of Cu(30)/ASA electrodes made with various ASA concentrations. The equivalent simple circuit model was used to fit the Nyquist curves. The impedance values of Rs, Rct, Cdl, and W were investigated in the electrode impedance analyses. The Cu(30)/ASA(0.005) electrode had the lowest Rs value, which was 16.69. Cu(30)/ASA(0.01), Cu(30)/ASA(0.02), Cu(30)/ASA(0.03), Cu(30)/ASA(0.04), and Cu(30)/ASA(0.05) electrodes had Rs values of 21.89, 18.55, 22.76, 27.14, and 31.08 respectively. Because they were performed under the same experimental conditions, the Rs values were close to one other, but there were minor differences. In the anodization process of the electrodes, an increase in Rs values occurred at increasing concentrations after 0.02 M ASA concentration. The Rct values of Cu(30)/ASA(0.005), Cu(30)/ASA(0.01), Cu(30)/ASA(0.02), Cu(30)/ASA(0.03), Cu(30)/ASA(0.04) and Cu(30)/ASA(0.05) electrodes were 17.74 Ω, 21.68 Ω, 23.49 Ω, 31.25 Ω, 33.46 Ω, and 38.89 Ω, respectively. While Rct values changed more in increasing concentrations after 0.02 M ASA concentration, semi-circle formation related to Rct formed in Nyquist curves was also observed clearly. The results showed that when the concentration of ASA added to the medium during the anodization process increases, charge transfer to the surface becomes more difficult. The Cdl values of Cu(30)/ASA(0.005), Cu(30)/ASA(0.01), Cu(30)/ASA(0.02), Cu(30)/ASA(0.03), Cu(30)/ASA(0.04), and Cu(30)/ASA(0.05) electrodes were 68.96e-6, 89.34e-6, 124.7e-6, 45.81e-6, 30.49e-6 and 23.35e-6, respectively. The W impedance values of Cu(30)/ASA(0.005), Cu(30)/ASA(0.01), Cu(30)/ASA(0.02), Cu(30)/ASA(0.03), Cu(30)/ASA(0.04) and Cu(30)/ASA(0.05) electrodes were 10.06e-3, 11.89e-3, 14.39e-3, 6.61e-3, 4.43e-3 and 2.96e-3, respectively. The highest diffusion rate ratio was obtained in Cu(30)/ASA(0.02) electrode. Similar to the downward trend in Rct values, W impedance values also decreased after 0.02 M ASA concentration. Excessive amount of ASA added to the medium affected the anodization negatively and slowed down the ion transfer and ion transfer rate.

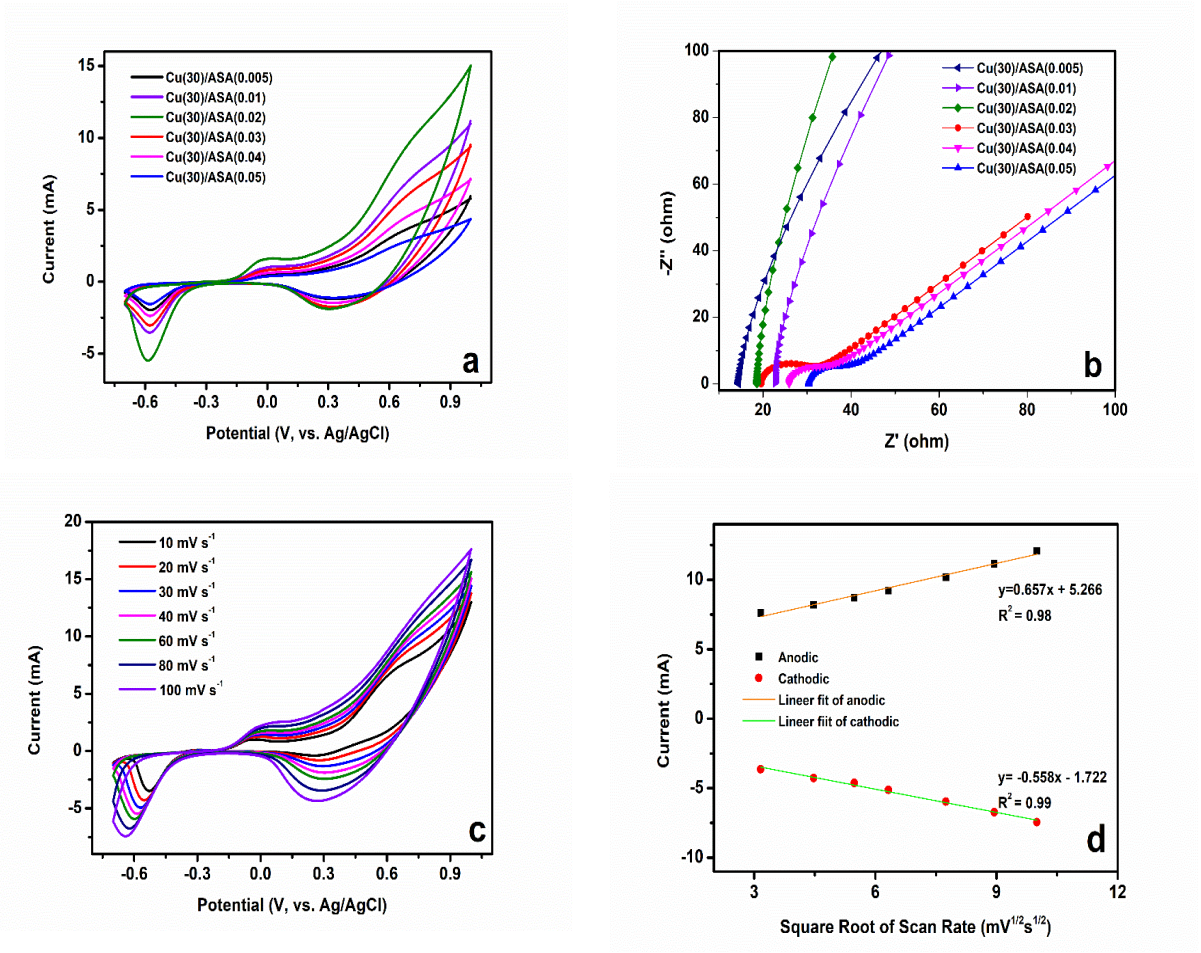

Figure 2: (a) CV of synthesized Cu(30) electrodes in the presence of various ASA concentration, (b) EIS spectra of synthesized Cu(30) electrodes in the presence of various ASA concentration, (c) Effect of scan rate on the CV of Cu(30)/ASA(0.02) in 5 mM of glucose at varying the scan rate from 10, 20, 30, 40, 60, 80 and 100 mV s^{-1}, (d) corresponding plot of peak current versus square root of scan rate for Cu(30)/ASA(0.02) electrode.

Figure 2c shows the rate performance of cyclic voltammetry in a three-electrode system with a platin counter electrode and an Ag/AgCl reference electrode in 0.1 M NaOH electrolyte solution in the presence of 5 mM glucose solution at scan rates of 10 to 100 mV s^{-1} with a voltage ranging from 0.7 V to 1.0 V. Peak currents gradually rose when scan rates were raised up to 100 mV s^{-1}. Redox current peaks were clearly visible in Figure 2d, and glucose oxidation at the anodic peak current (Ipa) altered proportionally with the scan rate. When the current linearity curves were plotted against the scanning speed, the findings revealed that two straight lines with good linearity were achieved, anodic and cathodic (R^2 a: 0.983, R^2 c: 0.998). It's clear that Cu(30)/ASA(0.02) has good electrochemical activity for glucose detection. The possible reaction mechanism was given below (26)(27):

$$CuO + OH^- \rightarrow CuO(OH) + e^- \quad (1)$$

$$CuO(OH) + e^- + \text{glucose} \rightarrow CuO + OH^- + \text{glucose acid} \quad (2)$$

The major processes occurring in CuO-based sensors are presented in equations (1) and (2) to allow electro-oxidation of glucose. The electro-oxidation of glucose by redox active ions (Cu^{2+}/Cu^{3+}) in the form of CuO/CuO(OH) complexes is a generally established non-enzymatic process. Furthermore, glucose sensing with a non-enzymatic CuO-based glucose sensor necessitates a medium with a high pH (13) (28).

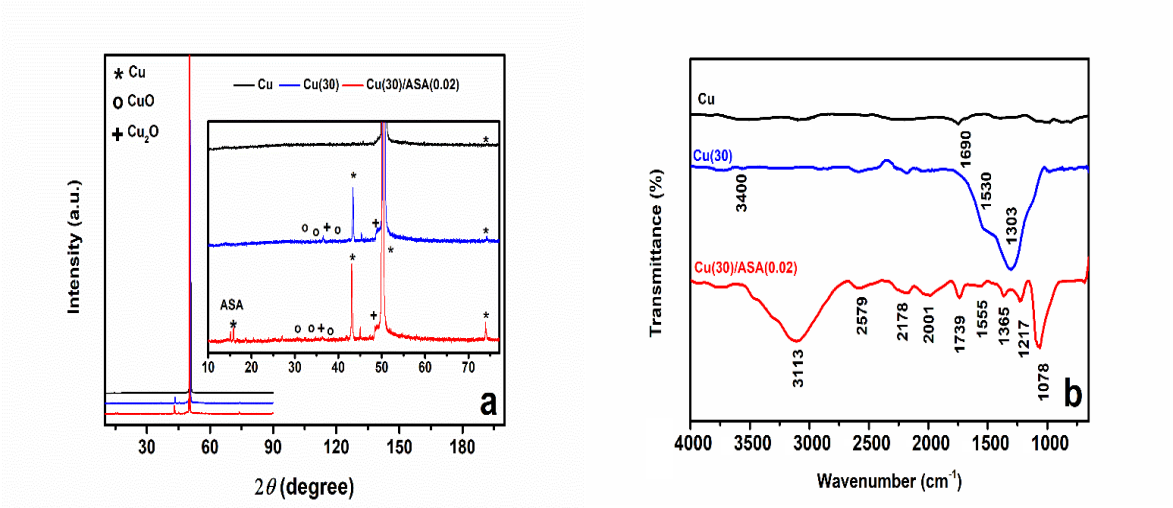

Figure 3: a) XRD patterns and b) FTIR spectra of the Cu, Cu(30) and Cu(30)/ASA(0.02) electrodes.

Cu, Cu(30), and Cu(30)/ASA(0.02) electrodes were examined using XRD analysis to investigate the crystal structure and phase composition, as shown in Figure 3a. At 2θ = 43.35, 50.47, and 74.16°, three prominent reflection peaks were found, indicating the (1 1 1), (2 0 0), and (2 2 0) crystal planes of the copper metal structure, respectively (JCPDS No. 02-1225) (29). An unknown peak was also observed at all three electrodes at 2-theta = 45.34°. Since the copper used in the experiments was not a high purity research grade product, it was possible for the material to contain unknown impurities. The different peaks were observed and defined in the XRD spectrum of Cu(30) grown on copper plate. The crystal structure and phase composition of the Cu(30) electrode can be linked to the cubic Cu substrate's (111), (200), and (220) planes. The copper metal corresponding peak observed in the sample may originate from copper under-layer or voids in the Cu(30) and Cu(30)/ASA(0.02) electrodes. The structure of monoclinic CuO (JCPDS no. 45-0937) and the structure of cubic Cu_2O could be the additional diffraction peaks besides Cu indicated with symbols (JCPDS no. 05-0667) (30,31).

The stretching vibrations of the O-H bond in air, molecular water adsorbed on the surface of Cu plate were characterized in the FTIR spectrum of Cu plate displayed in Figure 3b at 3407 cm^{-1} (32). Furthermore, a vibration of O-H bond was also observed around 1690 cm^{-1}, indicating that the associated hydroxyl groups were chemically poorly absorbed due to atmospheric molecular water (33). The formation of O_2 adsorption on CuO was confirmed by the formation of the intense υ(O–O) band around 1530 cm^{-1} (34). The variation of the intensity of the peaks with the anodization of copper can be attributed to the change in crystallinity. The C=O bond was attributed to the band at 1303 cm^{-1}, indicating that components from the electrolyte media were included into the formed oxide (26). A various peak forms were observed in the FTIR spectrum, which shows the structural change of the Cu(30)/ASA(0.02) electrode with the addition of aniline 2-sulfonic acid to the medium. The peak at 3113 cm^{-1} may be attributed to the interaction between the copper oxide and the N-H group of ASA, hydrogen bond formation between the copper oxide and the N-H group of ASA at the electrode surface (35).

For Cu(30)/ASA(002), the bands at 2579 cm^{-1}, 2178 cm^{-1}, and 2001 cm^{-1} were caused by aromatic C-H stretching C=O group was given to the band at 1739 cm^{-1}. The C=C stretching quinonoid and benzenoid rings of ASA were responsible for the bands at 1555 cm^{-1} and 1365 cm^{-1}, while the C-N stretching of the benzenoid units of ASA was relevant for the bands at 1217 cm^{-1} and 1078 cm^{-1} (18,19,35).

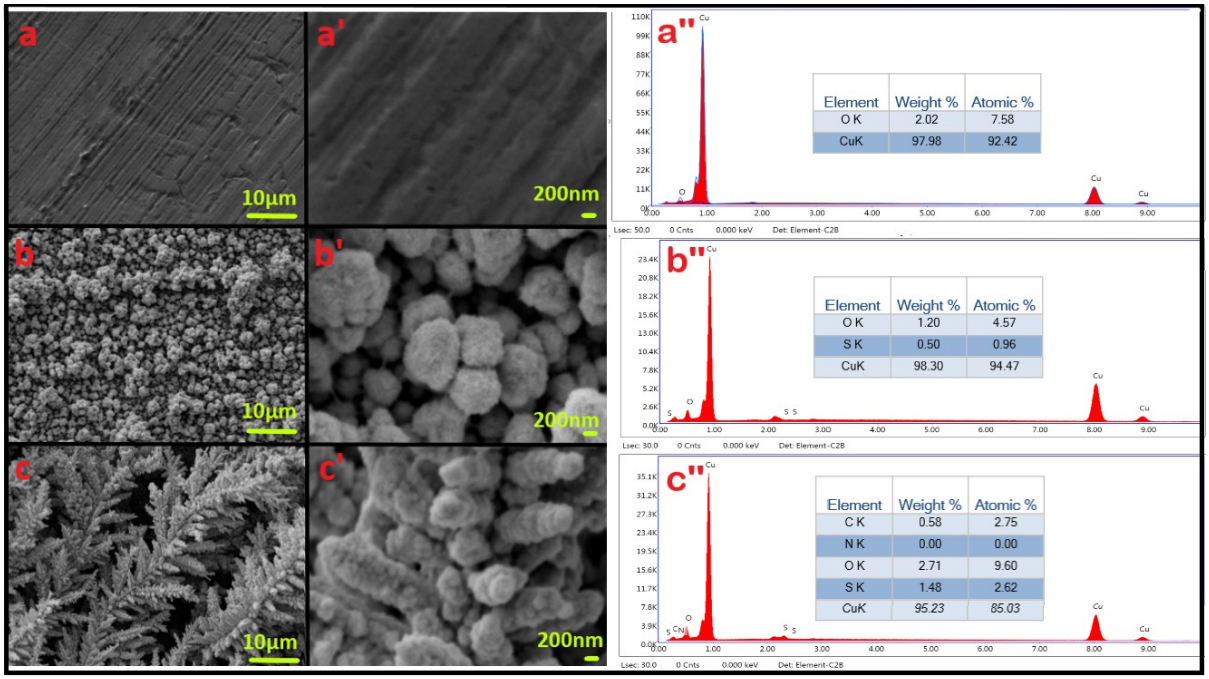

Figure 4: Comparison of the SEM images, EDS spectra for (a, a', a'')cCu electrode, (b, b',b'') Cu(30) electrode and (c, c',c'') Cu(30)/ASA(0.02) electrode.

The SEM images and EDS analysis of the surface of the copper-based electrodes were shown in Figure 4. Numerous CuO/Cu_2O microstructures coated uniformly agglomerates are shown in Figure 4 (b,b''). The homogeneous clusters were formed on the entire surface of the electrode and grain sizes are about ~0.1 µm. When the SEM image was examined at a higher magnification, it was seen that there were two different morphologies. The structures of needle with a diameter and length of about 200 nm and the other one was flower-like aggregates about a few microns in diameter in shown in the surface of Cu(30) electrode. As shown in Figure 4 (c,c''), interestingly, tree branch-shaped copper oxide structure observed in the presence of 0.02 M ASA concentration. When the SEM image was examined with a higher magnification, it was observed that there were nanoparticles 200 nm below the Cu(30)/ASA(0.02) electrode surface. When the SEM photographs are examined, the synthesized material exhibits an active rough structure at extremely nanoscale. The Cu(30)/ASA(0.02) electrode was much more porous, allowing electrooxidation to occur for the glucose sensor due to the availability of free interspace and increased surface area. It was in agreement with the electrochemical results that the Cu(30)/ASA(0.02) sensor showed a higher sensitivity than others.

The elemental distributions of the electrodes were determined by EDS measurement and the EDS spectrum of Cu, Cu(30) and Cu(30)/ASA(0.02) was presented in Figure 4 (a'',b''c'') and the percentage of elements was tabulated in the figures. EDS is an important technique for determining the atomic composition of elements in materials. EDS analysis also confirms that ASA interacts with the electrode surface during copper anodization process. The fundamental peaks of Cu and O are observed in all the EDS spectrums. The element S in the EDS spectrum of copper, which was also anodized in sulfuric acid electrolyte solution, originated from the electrolyte in the medium (36). Atomic percentage of Cu(30)/ASA(0.02) compared to atomic percentage of Cu(30), it was observed that the percentage of element S increased significantly with the addition of ASA. The atomic percentage of S increased from 0.96% to 2.62% as shown in Figure 4b'' and 4c''. Furthermore, EDS analysis showed Cu(30)/ASA (0.02) composition consisting of C, N, O, S and Cu elements included in the ASA added to the synthesis medium without other impurities.

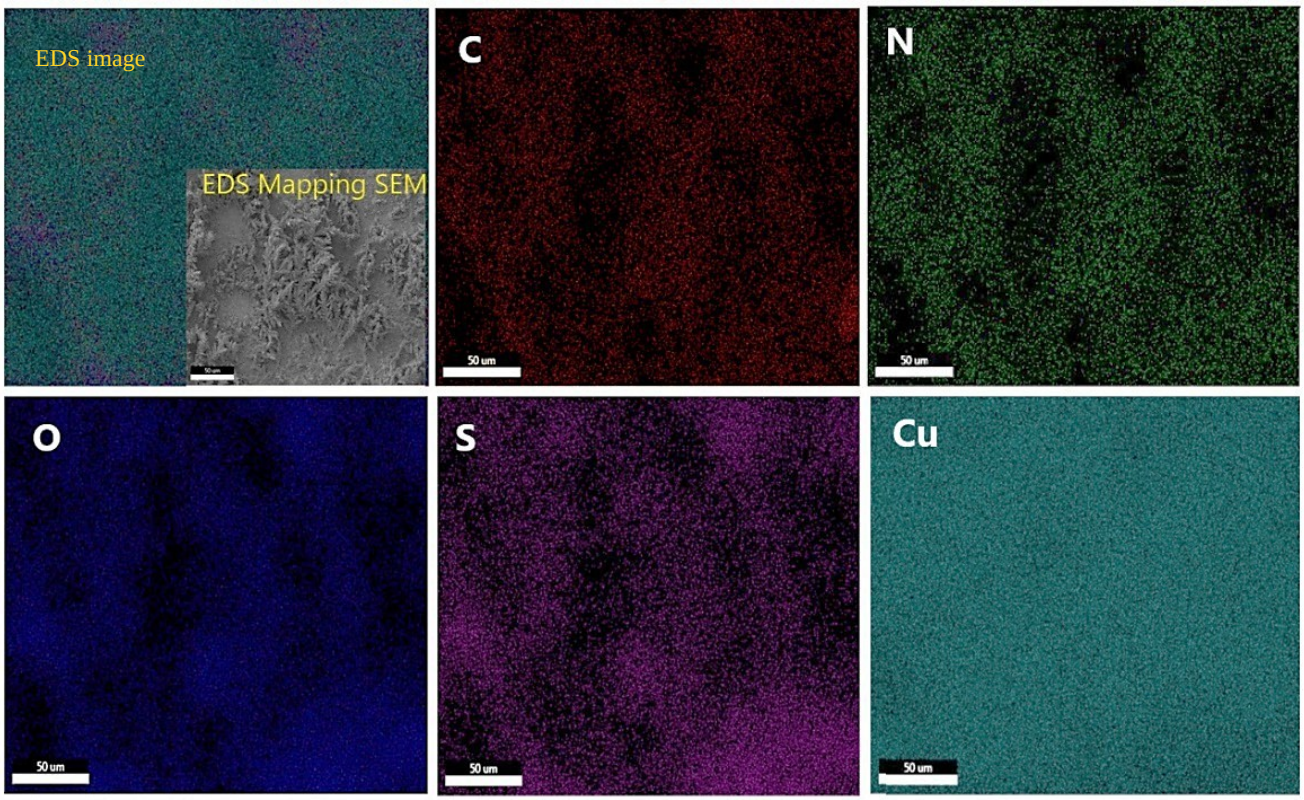

Figure 5: Elemental mapping of Cu(30)/ASA(0.02) electrode.

EDS mapping analyses of Cu(30)/ASA(0.02) are shown in Figure 5. In EDS mappings where the elements appear to be completely homogeneously distributed, it was observed that copper oxide and ASA showed good chemical interaction. The growth of copper oxides on certain active surfaces with the addition of ASA in the SEM morphology also proved this analysis.

Figure 6a demonstrated the electrocatalytic response of Cu(30)/ASA(0.02) electrode for the detection of the different concentrations of glucose (0.2, 0.5, 1.0, 2.0, 3.0, 5.0, 7.0 and 10.0 mM) in DPV technique (DPV parameters; step potential = 0.0050 V; modulation amplitude = 0.0250 V; modulation time = 0.20 s and interval time-0.5 s). Cu(30)/ASA(0.02) clearly exhibits a high degree of electrocatalytic activity for glucose detection. The size of the wave around 0.35 V to 0.65 V gradually increased as the glucose concentration raised for the Cu(30)/ASA(0.02) electrode. A good correlation was exhibited between glucose concentrations and peak currents (Figure 6b).

Typically, glucose oxidation peak current risen linearly with glucose concentration for values between 0.2 and 10 mM with correlation coefficient (R^2) as 0.998. The lowest detection limits for glucose (LOD) were found to be 0.826 µM (S/N=3) (Figure 6) (LOD = 3σ/S; the standard deviation and S is the sensitivity). Similarly, Cu(30)/ASA(0.02) was tested by cyclic voltammetry to examine glucose sensitivity. The glucose oxidation peak was seen at 0.35-0.65 V, and the oxidation current increased as the glucose concentration increased from 0.2 to 10.0 mM, as shown in Figure 6c. Table 2 shows the electrochemical sensor parameters for the glucose sensor, as well as prior publications using copper electrodes. It's worth noting that the Cu(30)/ASA(0.02) sensor's performance is comparable to that of prior investigations.

Some biological samples in the biological sample can be quickly oxidized at a positive potential, causing glucose detection to be interfered. As shown in Figure 7, the selectivity of the Cu(30)/ASA(0.02) electrode over glucose was investigated using various interfering species such as maltose, lactose, ascorbic acid, uric acid, lactic acid, and urea. Amperometric tests were used to analyse the electrolyte solution of 0.1 M NaOH. By adding 0.1 mM interfering agents and 2 mM glucose solution to a constantly stirred 0.1 M NaOH solution, the interaction of these electroactive biological samples was examined. As a result, in the presence of other biological species, the Cu(30)/ASA(0.02) electrode was better suited for glucose determination. This supports the idea that the Cu(30)/ASA(0.02) electrode's high surface area will give more sensitive selectivity for glucose detection under physiological settings, as it enhances selective glucose oxidation. Several factors are likely to have influenced this remarkable selectivity behaviour. First, because ASA reduces copper oxide agglomeration, the electrode material lasts longer. Second, tree branch-shaped copper oxide allows for

quick ion/electron transfer between the electrode and the electrolyte contact, resulting in improved sensing performance.

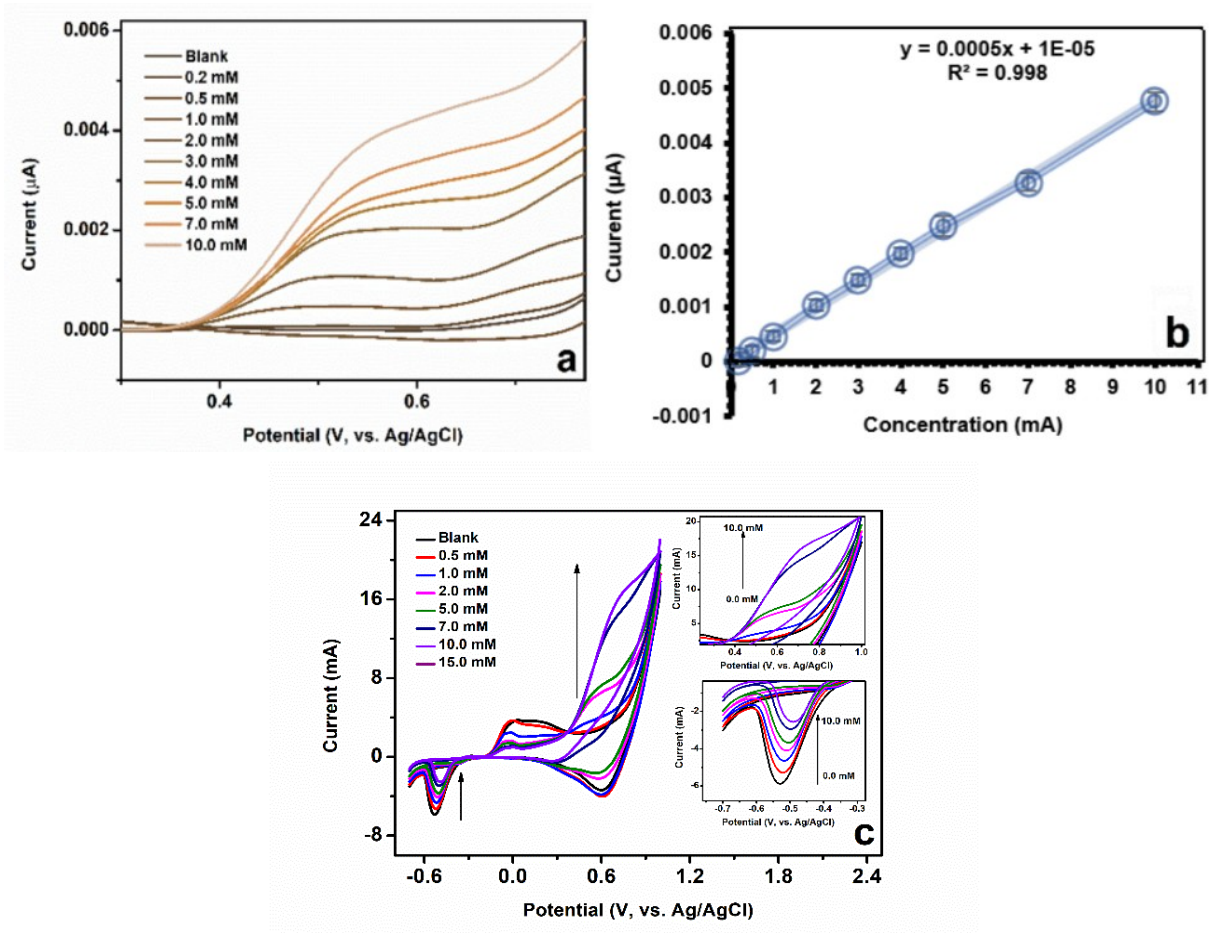

Figure 6: (a) Differential pulse voltammogram of Cu(30)/ASA(0.02) electrode in 1.0 M NaOH for values between 0.2 and 10 mM of glucose, (b) a plot of current density with respect to the concentration, (c) CV of Cu(30)/ASA(0.02) electrode in 1.0 M NaOH for values between 0.2 and 10 mM of glucose.

The sensor electrode's repeatability and stability were further tested using five separate electrodes and the addition of a 5.0 mM glucose solution in 0.1 M NaOH. The results demonstrate that the relative standard deviation value (RSD) was 2.41%, indicating that the sensor was reliable and repeatable. The sensor's stability was assessed over a 28-day period by assessing its sensitivity to 5.0 mM glucose. The sensitivity was tested every seven days after the same procedures were repeated and stored at room temperature. The electrode recovered 94 percent of the time, according to the results. The results show that it can be used in practical uses for most common analyses.

Glucose detection in real samples such as cherry juice, cola, and iced tea drinks was performed to assess the practical use of the Cu(30)/ASA(0.02) electrode. Drinks diluted with multiple applications of glucose standards were introduced to 0.1 M NaOH to determine glucose concentration in real samples. Figure 8 shows the result of the measurements (DPV parameters: step potential 0.0050 V, modulation amplitude 0.0250 V, modulation duration 0.20 s, and interval time 0.5 s.). Cherry juice, cola, and iced tea had average glucose concentrations of 4.3±0.19, 5.2±0.24, and 4.8±0.21 mM, with RSDs of 3.31%, 3.89%, and 3.49% respectively. The electrode was found to be capable of sensing glucose in both real samples and in different types of beverages.

Table 2: List of copper-based non-enzymatic glucose sensors.

Electrode materials	Analyte	Linear range	Limit of detection	Ref.
CuO/GCE	0.1 M PBS	5 µM–15 mM	1.42 µM	(26)
Copper-salen	0.5 M KCl	4.0–69 µM	1.2 µM	(37)
CuCo–CFs/Nafion/GC electrode	0.1 M NaOH	0.02–11 mM	1.0 µM	(38)
CuO/PANI-NF/FTO	0.1 M NaOH	0.25 µM to 4.6 mM	0.24 µM	(39)
CuO/NiO/PANI/GCE	0.1 M NaOH	0.02–2.5 mM	2.0 µM	(40)
CuO-U	0.1 M NaOH	1.0 µM to 10.0 mM	1.74 µM	(41)
CuS nanosheets/Cu_2O/CuO NWAs/Cu foil	0.1 M NaOH	0.002–4.1 mM	0.89 µM	(42)
CuO-C-dots	0.1 M NaOH	0.5–2.0 and 2.0–5.0 mM	200 µM	(43)
CuO-flower	0.1 M NaOH	0.001–1 mM	0.25 µM	(44)
CuO micro-/nanostructures	0.1 M NaOH	0.9–16 mM	20.0 µM	(45)
Cu(30)/ASA(0.02)	0.1 M NaOH	0.2–10.0 mM	0.83 µM	(This work)

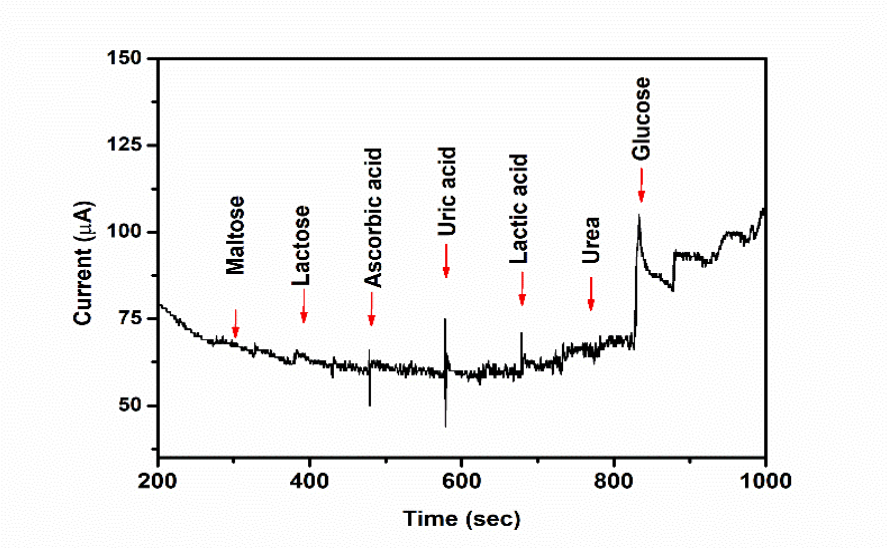

Figure 7: Amperometric response of the interference study of different samples in 0.1 M NaOH at potential 0.5 V.

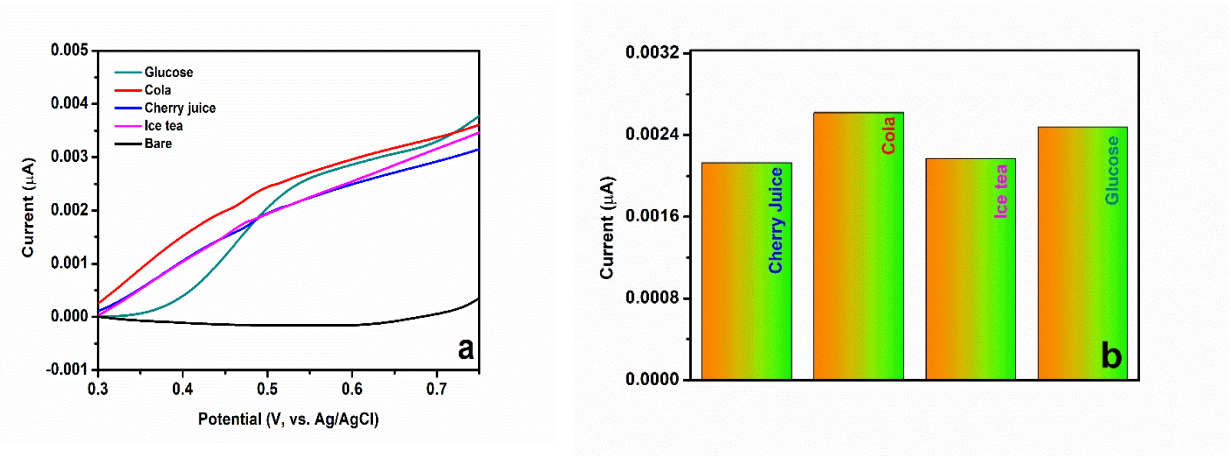

Figure 8: (a) DPV voltammogram, (b) the current density obtained DPV of different types of beverages in the real sample.

4. CONCLUSION

In this work, a new electrode material of Cu(30)/ASA(0.02) was synthesized and characterized for the non-enzymatic glucose sensor applications. In order to obtain a new electrochemical sensor for the prepared electrode, the effect of ASA added in the medium during the anodization of the copper foil was investigated for glucose. The electrode material was explored structurally and morphologically, as it provides a conductive path for quick electron/ion transfer to copper and facilitates harsh redox conditions by effectively increasing the active surface area. The electrode demonstrated an outstanding glucose sensing performance with acceptable sensitivity and a linear range analytical response, 0.2 to 10.0 mM, with a 0.826 µM limit of detection in DPV analysis for sensor application. Furthermore, the developed electrode has the potential to detect glucose in biological and food samples due to appropriate selectivity, stability, and great sensing performance in real beverages.

5. ACKNOWLEDGMENTS

M.B. Arvas especially thanks Prof. Dr. Yucel Sahin for his valuable contributions to this study.

6. REFERENCES

1. Yoo E-H, Lee S-Y. Glucose Biosensors: An Overview of Use in Clinical Practice. Sensors [Internet]. 2010 May 4;10(5):4558–76. Available from: <URL>.

2. Khor SM, Choi J, Won P, Ko SH. Challenges and Strategies in Developing an Enzymatic Wearable Sweat Glucose Biosensor as a Practical Point-Of-Care Monitoring Tool for Type II Diabetes. Nanomaterials [Internet]. 2022 Jan 10;12(2):221. Available from: <URL>.

3. Osuna V, Vega-Rios A, Zaragoza-Contreras EA, Estrada-Moreno IA, Dominguez RB. Progress of Polyaniline Glucose Sensors for Diabetes Mellitus Management Utilizing Enzymatic and Non-Enzymatic Detection. Biosensors [Internet]. 2022 Feb 22;12(3):137. Available from: <URL>.

4. Hassan MH, Vyas C, Grieve B, Bartolo P. Recent Advances in Enzymatic and Non-Enzymatic Electrochemical Glucose Sensing. Sensors [Internet]. 2021 Jul 8;21(14):4672. Available from: <URL>.

5. Malekzad H, Sahandi Zangabad P, Mirshekari H, Karimi M, Hamblin MR. Noble metal nanoparticles in biosensors: recent studies and applications. Nanotechnol Rev [Internet]. 2017 Jun 27;6(3):301–29. Available from: <URL>.

6. Barbee B, Muchharla B, Adedeji A, Karoui A, Kumar Sadasivuni K, Sha MS, et al. Cu and Ni Co-sputtered heteroatomic thin film for enhanced nonenzymatic glucose detection. Sci Rep [Internet]. 2022 May 7;12(1):7507. Available from: <URL>.

7. Pourbeyram S, Mehdizadeh K. Nonenzymatic glucose sensor based on disposable pencil graphite electrode modified by copper nanoparticles. J Food Drug Anal [Internet]. 2016 Oct 1;24(4):894–902. Available from: <URL>.

8. Yazar S, Kurtulbaş E, Ortaboy S, Atun G, Şahin S. Screening of the antioxidant properties of olive (Olea europaea) leaf extract by titanium based reduced graphene oxide electrode. Korean J Chem Eng [Internet]. 2019 Jul 25;36(7):1184–92. Available from: <URL>.

9. Kurtulbaş E, Yazar S, Ortaboy S, Atun G, Şahin S. Evaluation of the phenolic antioxidants of olive (Olea europaea) leaf extract obtained by a green approach: Use of reduced graphene oxide for electrochemical analysis. Chem Eng Commun [Internet]. 2020 Jul 2;207(7):920–32. Available from: <URL>.

10. Białas K, Moschou D, Marken F, Estrela P. Electrochemical sensors based on metal nanoparticles with biocatalytic activity. Microchim Acta [Internet]. 2022 Apr 2;189(4):172. Available from: <URL>.

11. Liu X, Cui S, Sun Z, Du P. Copper oxide nanomaterials synthesized from simple copper salts as active catalysts for electrocatalytic water oxidation. Electrochim Acta [Internet]. 2015 Apr 1;160:202–8. Available from: <URL>.

12. Arvas MB, Gencten M, Sahin Y. One-step synthesized N-doped graphene-based electrode materials for supercapacitor applications. Ionics (Kiel) [Internet]. 2021 May 5;27(5):2241–56. Available from: <URL>.

13. Mansuroglu A, Arvas MB, Kiraz C, Sayhan B, Akgumus A, Gencten M, et al. N-Doped Graphene Oxide as Additive for Fumed Silica Based Gel Electrolyte of Valve Regulated Lead Acid Batteries. J Electrochem Soc [Internet]. 2021 Jun 1;168(6):060512. Available from: <URL>.

14. Jiang D, Liu Q, Wang K, Qian J, Dong X, Yang Z, et al. Enhanced non-enzymatic glucose sensing based on copper nanoparticles decorated nitrogen-doped graphene. Biosens Bioelectron [Internet]. 2014 Apr 15;54:273–8. Available from: <URL>.

15. Zhang Y, Li N, Xiang Y, Wang D, Zhang P, Wang Y, et al. A flexible non-enzymatic glucose sensor based on copper nanoparticles anchored on laser-induced graphene. Carbon N Y [Internet]. 2020 Jan 1;156:506–13. Available from: <URL>.

16. Anand VK, Bhatt K, Kumar S, Archana B, Sharma S, Singh K, et al. Sensitive and Enzyme-Free Glucose Sensor Based on Copper Nanowires/Polyaniline/Reduced Graphene Oxide Nanocomposite Ink. Int J Nanosci [Internet]. 2021 Apr 10 [cited 2023 Feb 26];20(02):2150020. Available from: <URL>.

17. Phetsang S, Kidkhunthod P, Chanlek N, Jakmunee J, Mungkornasawakul P, Ounnunkad K. Copper/reduced graphene oxide film modified electrode for non-enzymatic glucose sensing application. Sci Rep [Internet]. 2021 Apr 29;11(1):9302. Available from: <URL>.

18. Yazar S, Arvas MB, Sahin Y. An ultrahigh-energy density and wide potential window aqueous electrolyte supercapacitor built by polypyrrole/aniline 2-sulfonic acid modified carbon felt electrode. Int J Energy Res [Internet]. 2022 May 9;46(6):8042–60. Available from: <URL>.

19. Arvas MB, Yazar S, Sahin Y. Electrochemical synthesis and characterization of self-doped aniline 2-sulfonic acid-modified flexible electrode with high areal capacitance and rate capability for supercapacitors. Synth Met [Internet]. 2022 Apr 1;285:117017. Available from: <URL>.

20. Sokolova MP, Bobrova N V., Dmitriev IY, Vlasov P V., Smirnov NN, Elyashevich GK, et al. Anticorrosion activity of aniline–aniline-2-sulfonic acid copolymers on the steel surface. Russ J Appl Chem [Internet]. 2016 Mar 15;89(3):432–8. Available from: <URL>.

21. Marioli JM, Kuwana T. Electrochemical characterization of carbohydrate oxidation at copper electrodes. Electrochim Acta [Internet]. 1992 Jun;37(7):1187–97. Available from: <URL>.

22. Li Z, Chen Y, Xin Y, Zhang Z. Sensitive electrochemical nonenzymatic glucose sensing based on anodized CuO nanowires on three-dimensional porous copper foam. Sci Rep [Internet]. 2015 Nov 2;5(1):16115. Available from: <URL>.

23. Wang G, Ding Y, Wang F, Li X, Li C. Poly(aniline-2-sulfonic acid) modified multiwalled carbon nanotubes with good aqueous dispersibility. J Colloid Interface Sci [Internet]. 2008 Jan 1;317(1):199–205. Available from: <URL>.

24. Şahin Y, Pekmez K, Yıldız A. Electropolymerization and in situ sulfonation of aniline in water–acetonitrile mixture containing FSO3H. Synth Met [Internet]. 2002 Nov;131(1–3):7–14. Available from: <URL>.

25. Şahin Y, Pekmez K, Yıldız A. Electrochemical preparation of soluble sulfonated polymers and aniline copolymers of aniline sulfonic acids in dimethylsulfoxide. J Appl Polym Sci [Internet]. 2003 Nov 21;90(8):2163–9. Available from: <URL>.

26. Sudha V, Murugadoss G, Thangamuthu R. Structural and morphological tuning of Cu-based metal oxide nanoparticles by a facile chemical method and highly electrochemical sensing of sulphite. Sci Rep [Internet]. 2021 Feb 9;11(1):3413. Available from: <URL>.

27. Abunahla H, Mohammad B, Alazzam A, Jaoude MA, Al-Qutayri M, Abdul Hadi S, et al. MOMSense: Metal-Oxide-Metal Elementary Glucose Sensor. Sci Rep [Internet]. 2019 Apr 2;9(1):5524. Available from: <URL>.

28. Strakosas X, Selberg J, Pansodtee P, Yonas N, Manapongpun P, Teodorescu M, et al. A non-enzymatic glucose sensor enabled by bioelectronic pH control. Sci Rep [Internet]. 2019 Jul 26;9(1):10844. Available from: <URL>.

29. Jayarathne RMHH, Pitigala PKDDP, Perera VP. Electronic and structural properties of Cu2O polycrystalline thin films grown on adhesive copper tape. Proc Tech Sess [Internet]. 2019 [cited 2023 Feb 26];35:31–8. Available from: <URL>.

30. He D, Wang G, Liu G, Suo H, Zhao C. Construction of leaf-like CuO–Cu 2 O nanocomposites on copper foam for high-performance supercapacitors. Dalt Trans [Internet]. 2017;46(10):3318–24. Available from: <URL>.

31. Volanti DP, Keyson D, Cavalcante LS, Simões AZ, Joya MR, Longo E, et al. Synthesis and characterization of CuO flower-nanostructure processing by a domestic hydrothermal microwave. J Alloys Compd [Internet]. 2008 Jul 14;459(1–2):537–42. Available from: <URL>,

32. Petrov T, Markova-Deneva I, Chauvet O, Nikolov R, Denev I. SEM and FT-IR spectroscopy study of Cu, Sn and Cu-Sn nanoparticles. J Univ Chem Technol Metall [Internet]. 2012;47(2):197–206. Available from: <URL>.

33. Diraz Uribe CE, Vallejo Lozada WA, Martinez Ortega F. Synthesis and characterization of TiO2 thin films dopedwith copper to be used in photocatalysis. Iteckne. 2013;10(1):16–20.

34. Abd-Elnaiem AM, Abdel-Rahim MA, Abdel-Latief AY, Mohamed AA-R, Mojsilović K, Stępniowski WJ. Fabrication, Characterization and Photocatalytic Activity of Copper Oxide Nanowires Formed by Anodization of Copper Foams. Materials (Basel) [Internet]. 2021 Sep 2;14(17):5030. Available from: <URL>.

35. Hesari Z, Shirkavand Hadavand B. Synthesis and Study on Conductivity of Urethane Acrylate/Polyaniline/CuO Nanocomposites. J Appl Chem Res [Internet]. 2018;12(4):66–77. Available from: <URL>.

36. Yazar S, Atun G. Electrochemical synthesis of tunable polypyrrole-based composites on carbon fabric for wide potential window aqueous supercapacitor. Int J Energy Res [Internet]. 2022 Aug 27;46(10):14408–23. Available from: <URL>.

37. Dadamos TRL, Teixeira MFS. Electrochemical sensor for sulfite determination based on a nanostructured copper-salen film modified electrode. Electrochim Acta [Internet]. 2009 Jul 30;54(19):4552–8. Available from: <URL>.

38. Li M, Liu L, Xiong Y, Liu X, Nsabimana A, Bo X, et al. Bimetallic MCo (M=Cu, Fe, Ni, and Mn) nanoparticles doped-carbon nanofibers synthetized by electrospinning for nonenzymatic glucose detection. Sensors Actuators B Chem [Internet]. 2015 Feb 1;207:614–22. Available from: <URL>.

39. Esmaeeli A, Ghaffarinejad A, Zahedi A, Vahidi O. Copper oxide-polyaniline nanofiber modified fluorine doped tin oxide (FTO) electrode as non-enzymatic glucose sensor. Sensors Actuators B Chem [Internet]. 2018 Aug 1;266:294–301. Available from: <URL>.

40. Ghanbari K, Babaei Z. Fabrication and characterization of non-enzymatic glucose sensor based on ternary NiO/CuO/polyaniline nanocomposite. Anal Biochem [Internet]. 2016 Apr 1;498:37–46. Available from: <URL>.

41. Mamleyev ER, Weidler PG, Nefedov A, Szabó DV, Islam M, Mager D, et al. Nano- and Microstructured Copper/Copper Oxide Composites on Laser-Induced Carbon for Enzyme-Free Glucose Sensors. ACS Appl Nano Mater [Internet]. 2021 Dec 24;4(12):13747–60. Available from: <URL>.

42. Wei C, Zou X, Liu Q, Li S, Kang C, Xiang W. A highly sensitive non-enzymatic glucose sensor based on CuS nanosheets modified Cu2O/CuO nanowire arrays. Electrochim Acta [Internet]. 2020 Feb 20;334:135630. Available from: <URL>.

43. Sridara T, Upan J, Saianand G, Tuantranont A, Karuwan C, Jakmunee J. Non-Enzymatic Amperometric Glucose Sensor Based on Carbon Nanodots and Copper Oxide Nanocomposites Electrode. Sensors [Internet]. 2020 Feb 2;20(3):808. Available from: <URL>.

44. Ashok A, Kumar A, Tarlochan F. Highly efficient nonenzymatic glucose sensors based on CuO nanoparticles. Appl Surf Sci [Internet]. 2019 Jul 1;481:712–22. Available from: <URL>.

45. Anu Prathap MU, Kaur B, Srivastava R. Hydrothermal synthesis of CuO micro-/nanostructures and their applications in the oxidative degradation of methylene blue and non-enzymatic sensing of glucose/H2O2. J Colloid Interface Sci [Internet]. 2012 Mar 15;370(1):144–54. Available from: <URL>.